Ocean Stommel Project

Jack Parkinson, Tom Donkovic, Emma Jewett

October 2023

1 Introduction

1.1 Ocean Currents

Ocean currents transport heat, salt, and nutrients globally through Thermohaline Circulation (THC). The THC is imperative to global energy and nutrient transport. Over recent years, the Atlantic Meridional Overturning Circulation (AMOC) is becoming increasingly weak[1]. One of the factors that can effect the AMOC is temperature; as of December 2022, NOAA and NASA have found that the Ocean is absorbing up to 90% of the heat from climate change, while only covering 70% of the globe's surface. The result of the heat influx in the oceans leads to a myriad of effects such as coral bleaching, thermal expansion, increased hurricane intensity, biochemistry effects, and hastened ice sheet melting[2]. In this project, we aim to explore the mechanisms that govern the AMOC, which would be affected by both increasing temperature as well as an increased freshwater flux from melting ice.

1.2 Stommel's Two-Box Model

In Henry Stommel's 1961 paper titled, "Thermohaline Convection with Two Stable Regimes of Flow," he investigated the density-driven convection flow due to differences in heat and salinity transfer[3]. In order to quantify this flow convection, Stommel created an idealized two-vessel experiment that connects two boxes of water through an upper overflow path and a lower capillary tube (fig. 1). In this model, there are two well-mixed vessels of water within two basins. The vessels are connected via a capillary of flow rate q and a resistance-adjacent hydraulic constant κ. The overflow channel allows the vessels to maintain a constant volume.
In this project, vessel one will represent a tropical Atlantic box. Vessel two will represent an northern Atlantic box resulting in a $T_1 > T_2$.

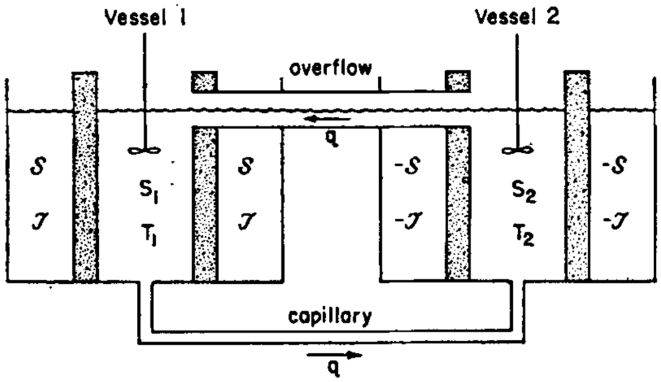

Figure 1: Stommel's two-box model with two separate wells of water surrounded by their own constant temperature and salinity reservoirs, connected by a capillary tube and an overflow tube.

1.2.1 Flow Rates and Densities

The rate of flow for water in the isolated two-box model can simply be described as the difference in densities between the vessels multiplied by a constant κ that describes the resistance to flow from the

capillary tube (Figure 1). Here, ρ_1 and ρ_2 have units kg/m^3 and q has units m^3/s, meaning κ has units kg $\cdot$ s / m^6.

$$q = \frac{1}{\kappa}(\rho_1 - \rho_2) \tag{1}$$

The density of seawater can be defined as

$$\rho = \rho_0 - \alpha_T(T - T_0) + \beta_S(S - S_0) \tag{2}$$

where α_T is defined as a thermal contraction coefficient and β_S is defined as a haline expansion. Equation (2) can be used to find $\rho_1 - \rho_2$ in terms of ΔT and ΔS:

$$\begin{aligned}\rho_1 - \rho_2 &= [\rho_0 - \alpha_T(T_1 - T_0) + \beta_S(S_1 - S_0)] - [\rho_0 - \alpha_T(T_2 - T_0) + \beta_S(S_2 - S_0)] \\ &= -\alpha_T T_1 + \beta_S S_1 + \alpha_T T_2 - \beta_S S_2 \\ &= \alpha_T(T_2 - T_1) - \beta_S(S_2 - S_1) \\ \rho_1 - \rho_2 &= \alpha_T \Delta T - \beta_S \Delta S \end{aligned} \tag{3}$$

and can used in equation (1) to find the flow rate in terms of ΔT and ΔS:

$$q = \frac{1}{\kappa}(\alpha_T \Delta T - \beta_S \Delta S) \tag{4}$$

The flow can be either dominated by temperature or dominated by salinity. Density is affected by both salinity and temperature. The warmer the water is, the less dense; however, warmer ocean water tends to have a higher salinity content. Increased salinity increases the density of water. As a result, when the flow is dominated by temperature, salinity is working against the flow. The AMOC is dominated by temperature at present in the Atlantic.
Flow is positive and controlled by temperature when the $\alpha_T \Delta T$ term outweighs the $\beta_S \Delta S$ term. To the contrary, flow is negative and controlled by the salinity when the opposite is true:

$$\begin{aligned} &\text{if } q > 0, \ \ \alpha_T \Delta T > \beta_S \Delta S, \quad \text{Temperature-driven} \\ &\text{if } q < 0, \ \ \beta_S \Delta S > \alpha_T \Delta T, \qquad \text{Salinity-driven} \end{aligned} \tag{5}$$

1.2.2 Equilibrium Points

The non-dimensional original two-box model finds equilibrium points by locating the intersections of a flow component with salinity-driven and temperature-driven density components. Recall figure 1 with well-mixed basins and two vessels, and set

$$T_1 = -T_2 = T$$

and

$$S_1 = -S_2 = S.$$

For a flow rate of $q = \frac{1}{\kappa}(\rho_1 - \rho_2)$ and a basin temperature and salinity of T_0 and S_0 respectively, the Stommel paper gives a time evolution of salinity and temperature [3]

$$\begin{aligned} \frac{dS}{dt} &= -|2q|S + d(S_0 - S) \\ \frac{dT}{dt} &= -|2q|T + c(T_0 - T) \end{aligned} \tag{6}$$

Where d is a salinity transfer coefficient and c is a temperature transfer coefficient[3]. In Stommel's model, the parameters are normalized and non-dimensionalized. The non-dimensionalized variables used are defined as:

$$\begin{aligned} &\tau = ct \quad \delta = \tfrac{d}{c} \qquad f = \tfrac{2q}{c} \\ &y = \tfrac{T}{T_0} \quad x = \tfrac{S}{S_0} \quad \lambda = \tfrac{c\kappa}{4\rho_0 \alpha_T T_0} \end{aligned} \tag{7}$$

The variable R is also defined, which acts as a measure of the ratio of the effect of salinity and temperature on the equilibrium density:

$$R = \frac{\beta_S S_0}{\alpha_T T_0} \tag{8}$$

Plugging the equations (7) and (8) into the differential system of equations (6) gives the dimensionless equations for the change in salinity (x) and temperature (y) over time (τ):

$$\begin{aligned} \frac{dy}{d\tau} &= 1 - y - \frac{y}{\lambda} \cdot |-y + Rx| \\ \frac{dx}{d\tau} &= \delta(1-x) - \frac{x}{\lambda} \cdot |-y + Rx| \end{aligned} \tag{9}$$

Steady states are identified when λf, a flow-related line intersects with $Rx - y$, related to the density due to both salinity and temperature in a temperature-driven two-box scenario:

$$\lambda f = \phi(f, R, \delta) = -\frac{1}{1+f} + \frac{R}{1+\frac{f}{\delta}} \tag{10}$$

1.2.3 Freshwater Flux

A freshwater flux, m, may also be introduced. In the North Atlantic box, freshwater from climate-change-induced ice cap and glacial melting can increase the water volume without changing the salt content, decreasing the salinity. The flux m could not be applied to Stommel's model using the system of equations (6), since it would only affect the salinity in the vessel two. The box will gain a net positive freshwater flux that decreases salinity. As a result, m would only be subtracted from $\frac{dS_2}{dt}$.

1.3 Purpose

The purpose of this project was to identify realistic parameters for coefficients c, d, α_T, and β_S to simulate the THC for the North Atlantic Ocean. Using those parameters, non-dimensionalized models will identify equilibrium points and explore the behavior of the two-box model. Dimensionalized models will explore equilibrium points and stable regimes. Noise in the form of an increased freshwater flux will then be added to the North Atlantic salinity differential equation to simulate melting glaciers and ice caps. From here, the stable flow rate can be computationally evaluated to determine the direction of the surface THC and any effect that glaciers melting impose to the present-day ocean currents.

2 Methods

2.1 Parameters

2.1.1 Coefficients β_S and α_T

The thermal contraction coefficient, α_T, and the haline expansion coefficient, β_S, have been derived from an equation of state for seawater. [4].

"The equation of state can be approximated using a linear function of temperature and salinity" [4]:

$$\sigma = \sigma_0 + \rho_{ref}[\beta_S(S - S_0) - \alpha_T(T - T_0)] \tag{11}$$

Where $\sigma = \rho - \rho_{ref}$, and $\rho_{ref} = 1000$ kg m^{-3}. While α_T and β_S change with pressure and temperature, this project will focus on surface layers and assume a pressure of 0 db. According to figure (3), $\alpha_T = 2.1 \times 10^{-4}$ and $\beta_S = 7.5 \times 10^{-4}$.

2.1.2 Coefficient c

To calculate the coefficient c, fundamental thermodynamics yields

$$c_p \rho V \frac{dT}{dt} = Q \tag{12}$$

For an arbitrary box of ocean water of volume V where c_p is the specific heat capacity at constant pressure of Atlantic seawater, ρ and V are the standard density and volume of seawater respectively, and Q in this case is the net heat transferred out of our system in Watts.

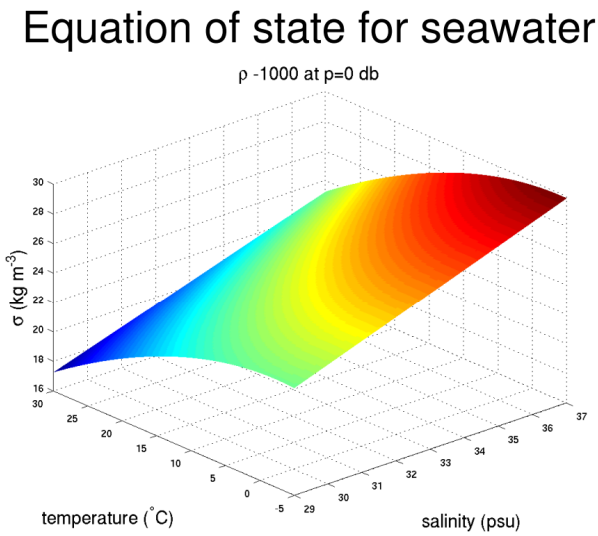

Figure 2: Equation of State provided by Markus Jochum. Salinity is provided in psu which has a one-to-one conversion to parts per thousand. The variable σ is a difference between the density and the reference density of pure water, $\rho_{ref} = 1000$ kg m $^{-3}$.

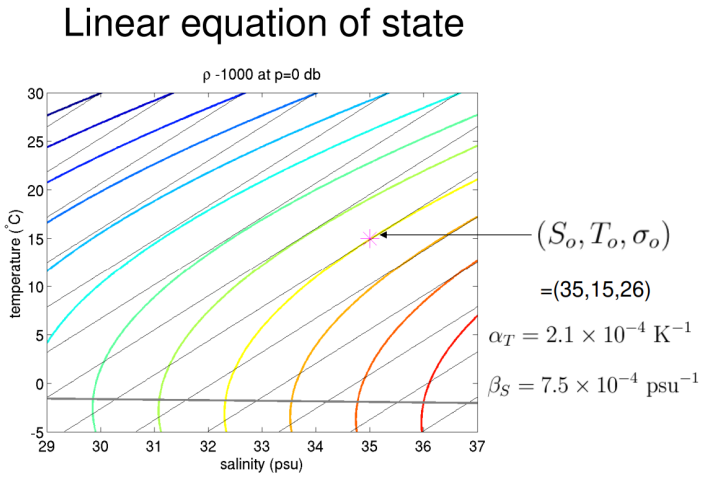

Figure 3: Equation of State approximation for 15 degrees Celsius provided by Markus Jochum[4].

Using the variable q to represent the the heat loss in Watts per square meter and the variables A and d to represent the lid area of the box in square meters and the depth of the box in meters, respectively, equation (12) can be rearranged to solve for dT/dt:

$$c_p \rho A d \frac{dT}{dt} = qA$$
$$\frac{dT}{dt} = \frac{q}{c_p \rho d} \tag{13}$$

Vessel one the tropical box closer to the equator with a water temperature set to 28 degrees Celsius. Vessel two is the northern box closer to the pole with a water temperature set to 6 degrees Celsius[5]. Due to a lack of surface radiation-measuring ocean buoys outside of the equatorial region, the outgoing radiation for both vessels will be assumed to be 409.6 W/m^2[6], the average outgoing surface long-wave radiation of the equatorial buoys.
Vessel one has a salinity of 36.5‰and temperature of 28 degrees Celsius, which corresponds closely to a specific heat capacity of $c_{p1} = 4001$ J/(kg C)[6, 7, 8, 9]. Vessel two has a salinity of around 34.5‰and temperature of 6 degrees Celsius, which corresponds closely to a specific heat capacity of $c_{p2} = 3984$ J/(kg C)[6, 7, 8, 9].

With resulting densities of $\rho_1 = 1023$ kg/m^3 and $\rho_2 = 1027$ kg/m^3[10] due to their temperatures and salinities, and box depths of $d = 1000$ m,

$$\frac{dT_1}{dt} = 1.00 \times 10^{-7}\text{C/s and } \frac{dT_2}{dt} = 1.00 \times 10^{-7}\text{C/s}$$

which are the c_1 and c_2 values per degree Celsius change. In this case, they are nearly equal to one another, differing by about 3.31×10^{-11}.

2.1.3 Coefficient d

Using a box with an arbitrary lid area of A in square meters, a depth of D meters, for a daily freshwater change of d in meters–either attributed to rainfall (positive) or evaporation (negative), a fixed volume of salt N, the rate of change of salinity over time due to the freshwater flux, using percent salinity, S can be found:

$$\frac{dS}{dt} = \frac{\Delta S}{Day} \tag{14}$$

The initial salinity can be defined as

$$S_i = \frac{N}{AD} \tag{15}$$

and the final salinity can be defined as

$$S_f = \frac{N}{A(D+d)} \tag{16}$$

Using equations (16) and (15), our ΔS is

$$\begin{aligned} S_f - S_i &= \frac{N}{A(D+d)} - \frac{N}{AD} \\ &= \frac{N}{Ad}(\frac{d}{D+d}) \\ \Delta S &= S_i(\frac{d}{D+d}) \end{aligned} \tag{17}$$

Original attempts to calculate this value yielded a value of magnitude 10^{-12}. Per correspondence with Markus Jochum, this value should be around $d = 10^{-10}$ s^{-1}[4], and will be used for both d_1 and d_2.

2.1.4 Hydraulic Constant κ

In the Stommel model the hydraulic constant κ represents the resistance to flow in the capillary connecting the two vessels. In the real-world application, it would represent the resistance to current. Several factors would influence the current flow in real life applications including but not limited to: isobaric surfaces, thermohaline and pressure gradients, ocean floor depth, and non-homogeneous velocities. Due to the complexity of estimating the hydraulic constant, there was a computational method devised to estimate it. First the solutions and phase diagrams were found for the non-dimensionalized code as seen in 3.2, with κ being used to update q every time step code using equation (1). Then κ was systematically increased until the system approached a non-divergent difference in temperature and salinity over time. This resulted in a κ value of 10^8m^3/kg s. This ensures a flow rate q with units 1/s that is dimensionally consistent with equation (18).

2.2 Non-dimensionalized Model

2.2.1 Rationale for Non-dimensionalization

The use of a non-dimensionalized code allows for observations on the ocean current behavior without accurate measurements. With so many complex real-world components and varying measurements with small location changes, there is an advantage of investigating the overall behavior of the flow and steady states without attempting to identify accurate parameters. However, the drawback is that the explicit values obtained have no real-world application.
One aspect of using the non-dimensionalized model with the symmetric temperature and salinity relationship allows the use of equation (10). The advantage of this is to see how many equilibrium points can be expected given a certain set of coefficients.

2.3 Dimensionalized Model

2.3.1 Dimensionalized Equations

Recall that in the process of non-dimensionlizing the temporal salinity and temperature equations, a symmetric relation of temperature and salinity of the reservoirs is defined where $T = T_1 = -T_2$ and where $S = S_1 = -S_2$ to derive two ODEs seen in equations: (6). Although this provides an avenue to analytically solve for equilibrium points, it results in non-dimensional results that can't easily be interpreted and generalized to the Atlantic Ocean. For example, the magnitude of T_1 is not necessarily equal to T_2 and the magnitude of S_1 is not necessarily equal to S_2 as is true in the non-dimmensional case, so a new set of ODEs were defined that allow for the dimensionalization of Temperature and Salinity solutions:

$$\begin{aligned}
\frac{dT_1}{dt} &= c_1(\mathcal{T}_1 - T_1) - (T_1 - T_2)|q| \\
\frac{dT_2}{dt} &= c_2(\mathcal{T}_2 - T_2) - (T_2 - T_1)|q| \\
\frac{dS_1}{dt} &= d_1(\mathcal{S}_1 - S_1) - (S_1 - S_2)|q| \\
\frac{dS_2}{dt} &= d_2(\mathcal{S}_2 - S_2) - (S_2 - S_1)|q|
\end{aligned} \tag{18}$$

Where the subscript 1 denotes the warm box, 2 denotes the cold box, $\mathcal{T}$ and $\mathcal{S}$ denote the reservoirs, T, S denote the boxes and the flow rate q is calculated from the difference in density of the two boxes divided by κ as given in equation (1).

2.3.2 Dimensionalized Code

All dimensionalized code referenced is in the attached 'Ocean_code.ipynb'.
First we initialized the dimensionalized parameters: $\alpha_T = 2.1 \times 10^{-4}$ s^{-1}, $\beta_S = 7.5 \times 10^{-4}$ psu^{-1}, $c = c_1 = c_2 = 1.00 \times 10^{-7}$ s^{-1}, $d = d_1 = d_2 = 1.00 \times 10^{-10}$ s^{-1}, $\kappa = 10^8$m^3/kg s , and our reservoir values $\mathcal{T}_1 = 28°$C, $\mathcal{S}_1 = 34.5$ psu and $\mathcal{T}_2 = 6°$C, $\mathcal{S}_2 = 36.5$ psu that were identified in Section 1. After these values were initialized, the equations from (18) were implemented into a ODE system `odesystem`, and solved with the SciPy built in `solve_ivp` function over a time range 0s to 3×10^8s or roughly 10 years. The `solve_ivp` works as a 4th order Runge-Kutta algorithim – meaning that at every time step 4 intermediary deviates are calculated for each of the four equations in equation (18), and then the solutions are updated using a weighted mean of these deviates.
It should also be noted that like in the non-dimensionalized code, there are two loops of `n1, n2` that represent the initial conditions of the salinity and temperatures of the two boxes. There is an if statement that evaluates if one of `n1, n2` is equivalent to 0 or 1 denoting one of the two boundary conditions: initial temperature and/or salinity of the two boxes are equal, and the initial temperature and/or salinity of the two boxes are equal to their reservoir. For the first initial boundary condition $(n_1, n_2 = 0, 0)$ a plot is created with time on the x axis and the proportion of the difference between box 1 and box 2 divided by the difference in reservoir 1 and reservoir 2 for both salinity and temperature. These plots help show how the salinity and temperature dynamics between the boxes and reservoirs change over time. Also in this boundary condition the basis for the phase diagram is created with every individual contour 'Z' value representing the difference between the densities of Box 1 and 2. Finally for every boundary condition, the trajectory of the salinity and temperature differences were plotted on the phase diagram to assess the stability and regime of the solution. If the final density data point for a boundary condition was 0 the line was shaded red to denote a temperature driven solution, otherwise it was shaded blue to denote a salinity driven solution.

2.3.3 Dimensionalized Noise

One purpose of this project was to add noise to this system to model melting of glaciers that introduces freshwater into the North Atlantic Ocean. Introducing freshwater to the system should decrease the salinity of the vessel two over time. Operating under the assumption this does not affect the differential equations representing the temperature of the cold reservoir, $\frac{dT_2}{dt}$, a constant positive parameter m can be implemented to model the change in salinity of the cold box:

$$\frac{dS_2}{dt} = d(\mathcal{S}_2 - S_2) - (S_2 - S_1)|q| - m \tag{19}$$

The actual value of m was tweaked until the system drastically changed for the first time as shown in Figure 10, which put the maximum convergent m = 10^{-8}psu/s, and a divergent m = 10^{-7}psu/s. The entire code was looped over three time for the three values of m : [0, 10^{-8} psu/s, 10^{-7} psu/s].

3 Results

In order to graphically visualize and asses the stability of the solutions, a contour plot was generated for both the non-dimensionalized and dimensionalized model, where the contour lines represent the difference in density between the two boxes (and is thus proportional to flow rate). The solutions of salinity and temperature for varying boundary conditions was plotted over the density difference contours. Density was chosen instead of flow rate because it eliminated the dimensional ambiguity of having a flow rate of inverse seconds for the dimensional case.

3.1 Non-dimensionalized Results

3.1.1 Evolution of Temperature and Salinity

To evaluate the temporal evolution of salinity and temperature in the non-dimensionalized model, we examined the system under varying initial conditions. Figure 6 illustrates that regardless of whether the model starts from a state of equilibrium (where both boxes have identical initial conditions) or from a state of maximum disparity, the system tends to stabilize at a temperature difference of 0.855 and a salinity difference of 0.055. This indicates that our model simulates a temperature driven flow.

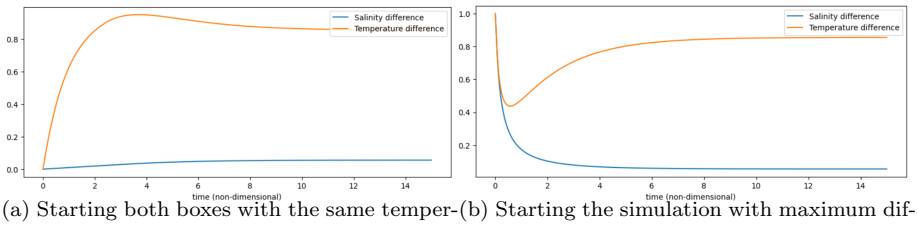

(a) Starting both boxes with the same temperature and salinity.

(b) Starting the simulation with maximum difference for both temperature and salinity.

Figure 4: Evolution of temperature and salinity difference with different initial conditions

3.1.2 Equilibrium analysis

Section 1.2.2 outlines the method for locating equilibrium points via equation 10. While the graphical analysis suggests the possibility of three real solutions, our phase diagrams only exhibit a single stable state. This implies that the system's stability cannot be solely determined by the analytical solution and intersection count and requires further investigation into the dynamics around these points.

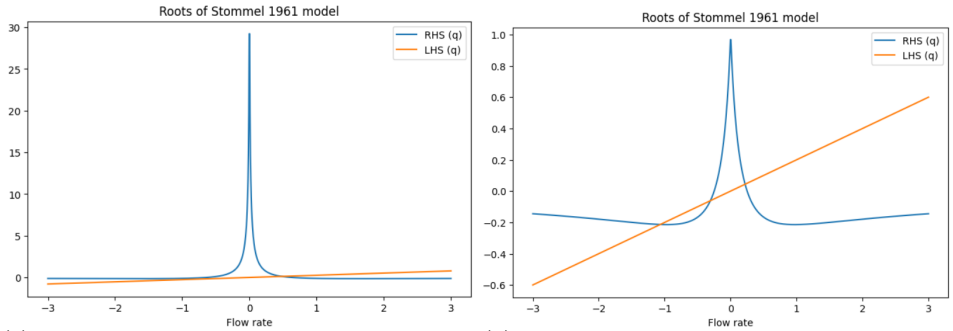

(a) Stommel's two box model using parameters from the Atlantic ocean shows one stable regime.

(b) The two box model using Stommel's original parameters leads to two stable regimes

Figure 5

3.1.3 Equilibrium Solutions

In continuation of the previous section and equilibrium analysis from section 3.2.2, we examine the stability of our model through phase contour plots. These plots are crucial for spotting stable states within the system. Our model, informed by Atlantic Ocean parameters, contrasts with the Stommel box model's two stable regimes. By adjusting the non-dimensional parameter κ from $10^{-2} - 10^{-5}$, we find that our model consistently shows only one stable equilibrium.

This finding indicates a more consistent state of oceanic behavior, suggesting that the Atlantic may not experience abrupt transitions in its current patterns based on the parameters used in our model.

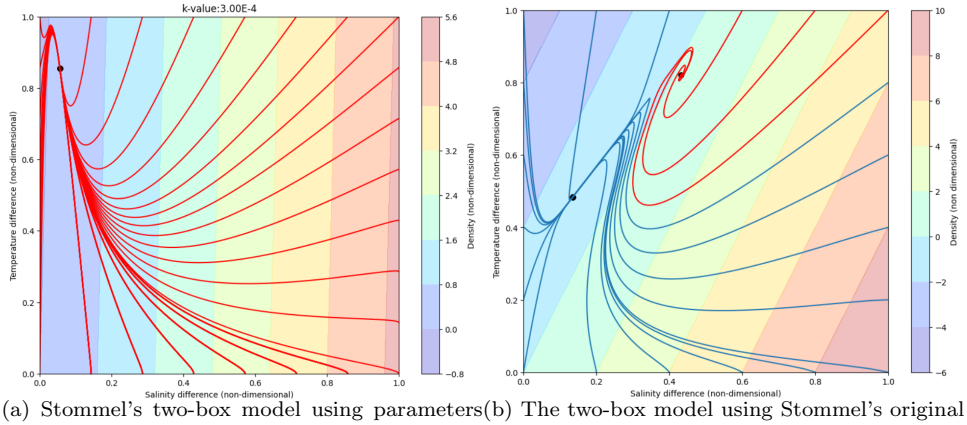

(a) Stommel's two-box model using parameters from the Atlantic ocean shows one stable regime.(b) The two-box model using Stommel's original parameters leads to two stable regimes

Figure 6

3.1.4 Result of Adding Freshwater Flux

Upon introducing a freshwater flux into the system and selecting a κ-value that approximates the threshold of dual stability, the dynamics of our model exhibit notable variations. The contour plot reveals trajectories indicative of temperature-driven flow (depicted in red) alongside a predominant number of salinity-driven trajectories (illustrated in blue).

If the Atlantic Ocean behaves similarly to our very simplified model, an ongoing incoming flux of freshwater which changes the salinity of the ocean, could potentially have detrimental effects in how the AMOC changes in the future.

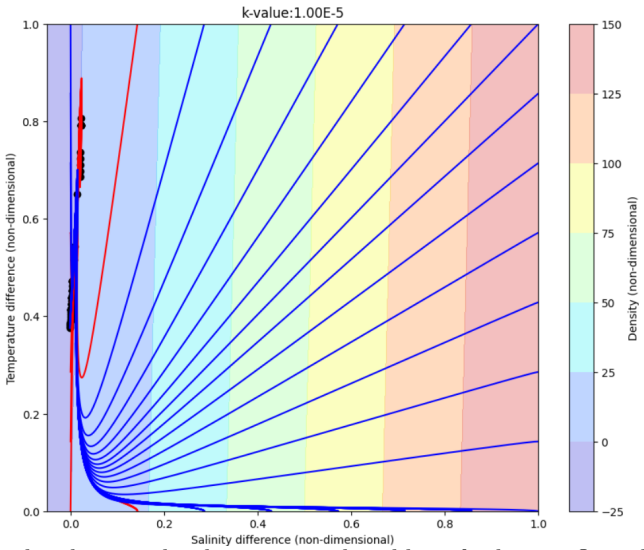

Figure 7: A phase contour plot showing the changes introduced by a freshwater flux which decreases salinity over time.

3.2 Dimensionalized Results

3.2.1 Temperature and Salinity Change Over Time

In order to understand how the temperature and salinity changes over time for our dimensionalized model, we should call our ODE solver with the dimensionalized parameters on meaningful initial conditions. For this purpose the most useful initial conditions could be boundary conditions where 1) the boxes are equal in temperature and salinity to their respective reservoirs and 2) where the boxes are the same temperature and salinity halfway in-between the reservoirs.
The first of these initial conditions can be set as: $T_1[0] = \mathcal{T}_1$, $S_1[0] = \mathcal{S}_1$, $T_2[0] = \mathcal{T}_2$, $S_2[0] = \mathcal{S}_2$. This system simulates the starting configuration that the box 1's salinity and temperature is equal to reservoir 1 and that box 2's salinity and temperature is equal to reservoir 2. This was simulated as shown in Figure 8a, and we over time the salinity difference between the two boxes approaches approximately 0, while the temperature difference approaches a ratio of 0.7 relative to the difference in the reservoir temperatures. This indicates that over a large amount of time, the salinity of the boxes become equivalent while the temperatures maintain a constant difference. We can then set a second system which has the initial conditions: $T_1[0] = T_2[0] = \frac{1}{2}(\mathcal{T}_1 + \mathcal{T}_2)$, $S_1[0] = S_2[0] = \frac{1}{2}(\mathcal{S}_1 + \mathcal{S}_2)$. These conditions represent an initial configuration where the boxes are the same temperature and salinity halfway in-between the reservoirs. The resulting graph figure 8b shows that the salinity difference between the two boxes stays 0 while the temperature difference approaches a constant value that looks roughly the same as in figure 8b. From these graphs we can expect that for our parameters the dimensionalized two-box model is completely temperature-driven as the salinity differences approaches zero for large time intervals. But a more exhaustive analysis is needed with the help of phase diagram.

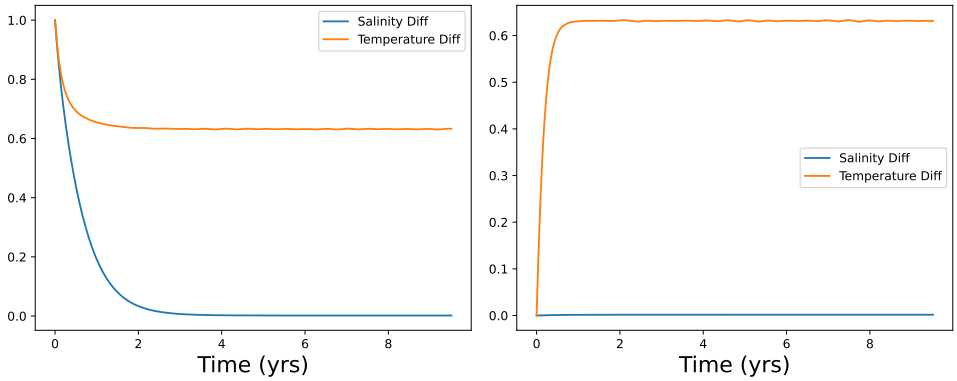

(a) Initial Conditions: Box1, Box2 = Res1, Res2 (b) Initial Conditions: Box1 = Box2

Figure 8: Graphs of salinity and temperature over time for two boundary conditions. The x-axis is time in years, and the y-axis is the ratio of the difference of box1 and box2 over the difference in reservoir value (for both salinity and temperature)

3.2.2 Phase Diagram / Equilibrium Solution

The results shown in figure 9 demonstrate that all initial boundary conditions converge on a steady flow rate with a salinity difference of 0.00342 psu and a temperature difference of 13.9 ° C. The final difference in density is positive, meaning the cold box maintains a higher density than the warm box and thus the flow rate is defined as temperature-driven. Like the non-dimensionalized case there is only one equilibrium solution which all initial conditions converge to.

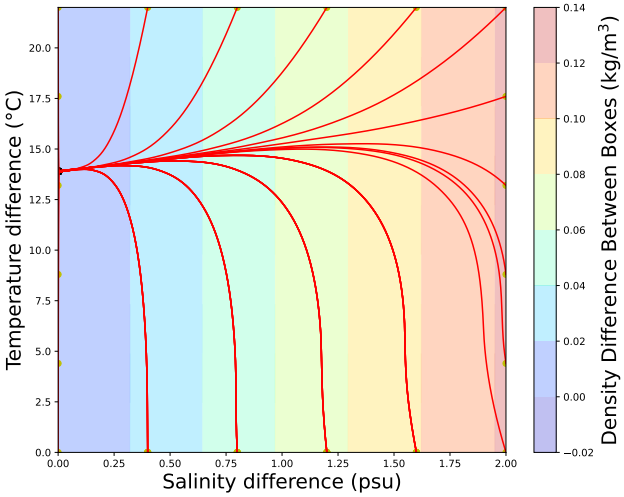

Figure 9: Contour plot of solutions to the differential equations from different boundary conditions with the contour values representing the difference in vessel/box densities (proportional to flow rate). The x-values of the solutions correspond to salinity difference between boxes while the y-values correspond to difference in temperature. The dark black point represents the final temporal solution while the faint yellow dots represent the initial conditions. The solutions are red to designate temperature-driven solutions, and blue would have denoted salinity-driven solutions.

3.2.3 Adding noise

A positive constant parameter m was subtracted at each time step as shown in equation (19). As discussed earlier, this is to simulate an influx of fresh water. The parameter m was tweaked until it reached a value that completely changed the equilibrium point from temperature-driven to salinity-driven. As seen in figure 10, when $m = 10^{-8}$ psu/s the model was still temperature driven with a positive flow rate, but when m was increased to 10^{-7} psu/s the influx of fresh water was so great that not only did the flow rate switch to salinity-driven, but the final salinity equilibrium point had a difference in salinity of the two boxes that was greater than the initial difference in salinity. This suggests that in order for our system with our defined parameters to have a salinity-driven solution, there has to be an incoming flux that changes the salinity of the system faster than can be equalized by the flow rate, otherwise, it is guaranteed to be temperature-driven. It also implies that the equilibrium solution is very stable for freshwater flux rates up to $m = 10^{-8}$ psu/s.

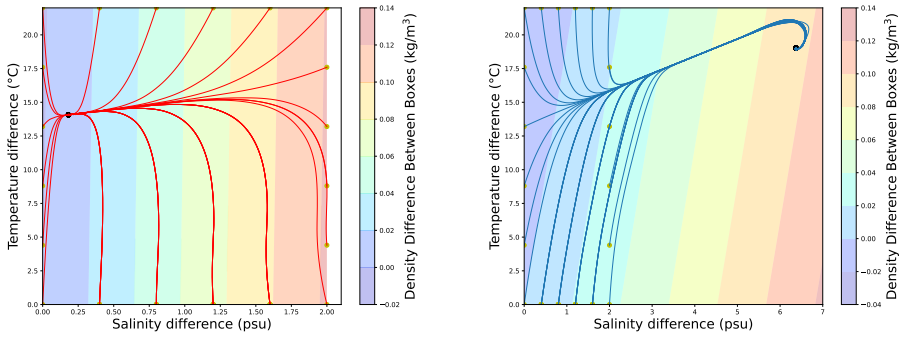

(a) $m = 10^{-8}$psu/s (b) $m = 10^{-7}$psu/s

Figure 10: Phase contour plots for two different m-values representing glacier melting rates. The left plot has an m value of 10^{-8}psu/s and demonstrates the largest magnitude for m before the system turns into a salinity-driven solution with a negative flow rate as shown in (b) with an $m = 10^{-7}$psu/s.

4 Interpretation

After running dimensionalized simulations of the two box model we can generalize our results to the the convective Atlantic ocean currents. Our results showed an equilibrium point for all of our starting boundary conditions with a positive flow rate that is temperature driven as shown in Figure 9. This means that our two-box model after a long period of time reaches a steady balanced flow rate which is directed from the warm box to the cold box on the upper overflow and is directed in the opposite direction on the bottom capillary. Generalizing this to the Atlantic, we would expect a Northward travelling surface current from the Equator to the North Atlantic and a Southward travelling deep ocean current travelling from the North Atlantic to the Equator. We can compare our predictions to the Atlantic currents in NASA's Thermohaline Ocean Circulation map (Figure 11), and we see that as we predicted there is a warm Northward travelling surface current and a Southward deep cool sea ocean current.

We can also generalize our findings from noise perturbations to the Atlantic Ocean and to see how melting glaciers would affect the direction of the Atlantic currents. Specifically we found that if the m in equation (19) was greater than 10^{-7}psu/s then the flow rate would reverse and become salinity driven as shown in figure 10. Generalizing this to the Atlantic would mean that if the glaciers were to melt at a rate expelling a salinity change at a rate of 10^{-7}psu/s over the course of 10 years then the current directions in the Atlantic ocean would switch direction meaning there would be a cold surface current from the North Atlantic to the Equator and a deep sea cold warm current from the Equator to the North Atlantic. However this is ignoring other non-Thermohaline Ocean currents such as the Gulf stream that may prolong or even negate the change from temperature driven to salinity driven. Future work could be directed towards modelling the potential rate and volume of possible Glacier melting and to see how realistic the m value of 10^{-7}psu/s in order to see how plausible it is that the Atlantic Ocean can change regimes to a Salinity Driven circulation pattern.

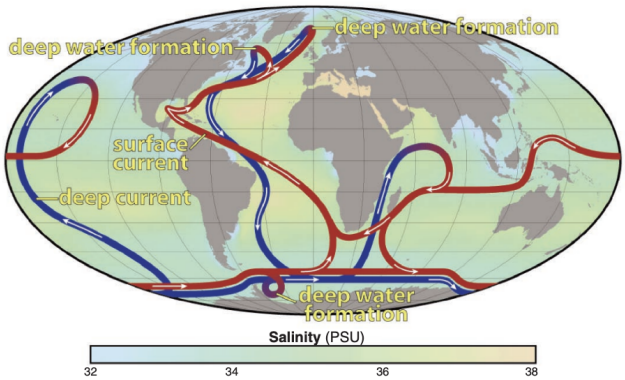

Figure 11: A map of the Thermohaline Ocean Circulation by Nasa[12]. In the figure the red lines denote warm currents, the blue lines represent the cold currents and the arrows on the lines denotes the direction the currents are travelling in.

5 Conclusion

The Atlantic Meridional Overturning Circulation (AMOC) might be one of the most important ocean currents for our climate system and simultaneously one of the most vulnerable tipping points in climate change discussions in the last few years. The possibility of a two-regime system was already shown in the 1961 paper "Thermohaline Convection with Two Stable Regimes of Flow" from Stommel which was used as the basis in this paper. Two ways of applying the two box model were developed and analyzed to approximate a simplified Atlantic ocean.
A non-dimensionalized model with realistic parameters has allowed us to explore a generalized system without being constrained by full-scale physical measurements. A second dimensionalized model was used to incorporate previously calculated and measured parameters by other groups.
The results of both models showed and agreed that with the chosen parameters only one stable regime exists in the simplified box model of the Atlantic ocean. The temperature driven flow seems to, no matter the distribution of salinity and temperature between the two boxes, always be the main deciding factor of the flow.

One factor that we hypothesized could disturb the balance in the Atlantic Ocean is the freshwater flux from the glaciers in Greenland induced by the rapid warming of Earth's climate.
To simulate this man-made phenomenon both models included a freshwater flux that starts at zero and linearly increases with time. The non-dimensionalized model does not show two definite stable regimes but introduces the possibility for salinity-driven flow under the right circumstances.
On the other hand, the dimensionalized model shows that if the freshwater flux leads to a change of $10^{-7}\frac{psu}{s}$ that a salinity driven flow is unavoidable in this simplified two box model of the Atlantic Ocean.

Further research has to be conducted to get more insight into the complex system we call the AMOC. Future work could entail research about how the freshwater flux from Greenland changes the salinity levels in the Atlantic Ocean or how to more realistically simulate the ocean currents induces by the density differences, especially the resistance κ to those currents. Another interesting subject to focus and improve on is to more accurately derive a system that accounts for both the inward flux from the glaciers and ice caps as well as the outward flux from the equator region.

In light of our findings, we underscore the critical importance of continued research into the AMOC's dynamics. It is imperative that the scientific community, policymakers, and the public collaborate to deepen our understanding of these complex systems. Such concerted efforts are essential to mitigate the risks associated with potential shifts in oceanic circulation patterns and to safeguard our climate's future stability.

References

[1] Walsh, J. (2019). The ocean and climate change: Stommel's conceptual model. *CODEE Journal, 12(1)*, 11-30. https://doi.org/10.5642/codee.201912.01.03

[2] NASA. (2023, August 2). *Ocean heat content.* NASA. https://climate.nasa.gov/vital-signs/ocean-warming/

[3] Stommel, H. (1961). Thermohaline convection with two stable regimes of Flow. *Tellus, 13(2)*, 224-230. https://doi.org/10.1111/j.2153-3490.1961.tb00079

[4] Jochum, M. (2023, October 11). Climate Physics Project.

[5] US Department of Commerce; NOAA; National Environmental Satellite Data and Information Service; Office of Satellite and Product Operations. (2012, February 14). *NOAA's office of satellite and product operations.*https://www.ospo.noaa.gov/Products/ocean/sst/contour/

[6] Wild, M., Folini, D., Hakuba, M. Z., Schär, C., Seneviratne, S. I., Kato, S., Rutan, D., Ammann, C., Wood, E. F., & König-Langlo, G. (2014). The energy balance over land and Oceans: An assessment based on direct observations and CMIP5 Climate models. *Climate Dynamics, 44*(11–12), 3393–3429. https://doi.org/10.1007/s00382-014-2430-z

[7] NASA salinity: SMAP RSS Maps. (n.d.). https://salinity.oceansciences.org/smap-salinity.htm

[8] Reverdin, G., Kestenare, E., Frankignoul, C., & Delcroix, T. (2007). Surface salinity in the Atlantic Ocean (30°S–50°N). *Progress in Oceanography, 73*(3–4), 311–340. https://doi.org/10.1016/j.pocean.2006.11.004

[9] Millero, F. J., Perron, G., & Desnoyers, J. E. (1973). Heat capacity of seawater solutions from 5° to 35°C and 0.5 to 22‰ chlorinity. *Journal of Geophysical Research, 78(21)*, 4499–4507. https://doi.org/10.1029/jc078i021p04499

[10] UNESCO (1981) Tenth report of the joint panel on oceanographic tables and standards. *UNESCO Technical Papers in Marine Science*, Paris, 25 p

[11] Hvidberg, C. S. (2023, September). Stommel. *Earth and Climate Physics.* Copenhagen; Copenhagen University.

[12] NASA. (Year). Ocean Surface Topography Mission/Jason-2. *Publication Title or Report Name.* Retrieved from https://eospso.nasa.gov/sites/default/files/publications/OSTMbrochure20081009.pdf